Controlling the Magnetic Ground State in $Cr_{1-x}V_x$ Films

O. Krupin,[1,2] Eli Rotenberg,[1] and S. D. Kevan[2]

[1]6-2100, Advanced Light Source, Lawrence Berkeley National Laboratory, Berkeley, California 94720, USA
[2]Department of Physics, University of Oregon, Eugene, Oregon 97403, USA

(Received 23 June 2007; published 5 October 2007)

We demonstrate the ability to control the magnetic phase diagram of $Cr_{1-x}V_x(110)$ thin films grown on a W(110) substrate. Using angle-resolved photoemission, we have mapped paramagnetic and commensurate and incommensurate antiferromagnetic phases as a function of temperature, film thickness, and composition. We show that surface-localized electron states play a key role in the observed phase behaviors and suggest from this that it might be possible to control the magnetic phase by applying an external electric field.

DOI: 10.1103/PhysRevLett.99.147208 PACS numbers: 75.30.Fv, 71.18.+y, 79.60.−i

Electric field controlled magnetization in magnetic semiconductors [1–3] will allow useful functionality to be implemented in spintronic devices. Analogous control in metallic films would have a similarly important impact, but strong electrostatic screening severely limits the ability to control a metal's electron states and magnetization. An alternative is to use an external field to modify the surface electronic structure in a thin metal film. If the surface electronic structure is coupled to the thin film magnetization through its impact on the ground state magnetic periodicity or the magnetic surface anisotropy, for example, then external control might be achieved. We explore the possibility of accomplishing this in a model system, $Cr_{1-x}V_x(110)$ thin films grown on a W(110) substrate. These can adopt paramagnetic (P), commensurate (C) antiferromagnetic, and incommensurate (IC) spin density wave (SDW) ground states depending on film composition (x), thickness (d), and temperature (T). Since the influence of an electric field on the surface electronic structure is likely to be small, it is important to tune the system so that control over the magnetic state can be maximized. We have measured part of the three dimensional (x, d, T) phase diagram using angle-resolved photoemission spectroscopy (ARPES). We find a significant change of the surface electronic structure and an approximately uniform shift of the magnetic phase diagram upon adsorbing a small amount of hydrogen on the outer surface. The modest change in the surface dipole layer associated with hydrogen adsorption suggests that similar control might be achieved using a field-effect geometry.

Chromium metal displays rich and fascinating physics when alloyed or confined to thin film structures [4–7]. This richness derives from many low energy degrees of freedom—SDW phase and amplitude, incommensurability, propagation direction, and spin orientation—that are dramatically impacted by confinement, strain, alloying, defects, and interfacial exchange interactions. Most thin film studies have probed (100)-oriented films in which quantization of the SDW across the film thickness affects the SDW phase diagram [8–16]. Chromium films with a (110) orientation have been less often studied but are potentially very interesting since interlayer magnetic exchange and SDW quantization are not relevant [17–20]. Weaker energetic interactions can then dominate phase behaviors, and the potential for external control is enhanced. ARPES is exquisitely sensitive to SDW periodicity and also probes the Fermi surface nesting that is a key aspect of the SDW energetics [21]. Using wedge-shaped thickness and alloy composition profiles allows systematic variation of thermal and nonthermal parameters, and the full (x, d, T) phase diagram can be mapped.

ARPES experiments were performed on beam line 7.0.1 at the Advanced Light Source using procedures generally described previously [21]. $Cr_{1-x}V_x$ films were grown epitaxially on a W(110) substrate in the form of double composition or thickness wedges [see Fig. 1(a)] by room temperature coevaporation with a spatially-varying vanadium flux, followed by rapid annealing to ~800 K. We assume that surface segregation is not a problem during the room temperature evaporation. By measuring the V $3p$ and Cr $3p$ core level intensities as a function of position on the

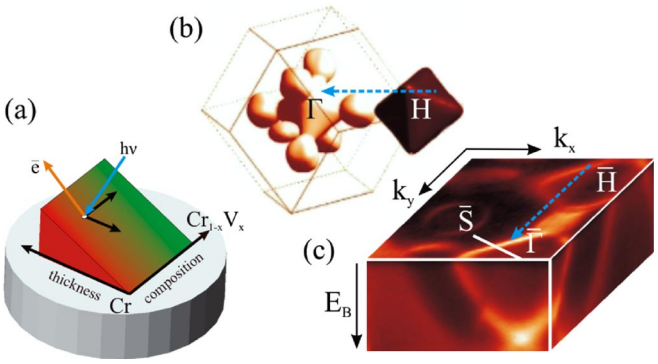

FIG. 1 (color online). (a) Schematic of the thickness-composition double wedge used in these experiments. (b) Calculated bulk chromium Fermi surface, showing the Γ-centered electron octahedron nested with the slightly larger H-centered hole octahedron. (c) 3D ARPES band map in the Γ-N-P-H plane of the bulk Brillouin zone, showing the dispersion of the bands that form the nested electron and hole Fermi surface octahedra.

wedge, we were able to monitor any change in the alloy composition after the annealing step. We found that this post-annealing step did not lead to measurable surface segregation of either alloy component, as long as the annealing temperature does not exceed necessary minimum value as judged from quality of photoemission spectra. d and x varied linearly from 0.8 to 15 nm and from 0.00 to 0.10, respectively, over the 5 mm substrate plane in orthogonal directions. We scanned the 50 μm focus of the soft x-ray photon beam along the film to study the x- and d-dependence of the electronic structure. The base pressure was 2×10^{-11} Torr, which increased to 2×10^{-10} Torr during evaporation. At a sample temperature T = 20–40 K, saturation hydrogen coverage could be achieved by exposing the film to an H_2 partial pressure of $\sim 5 \times 10^{-9}$ Torr for 400 sec. Films displayed both strong surface states and quantization of those bulk states having significant perpendicular dispersion, ensuring cleanliness and atomic flatness of the interfaces.

Nesting along $\langle 001 \rangle$ directions between flat faces of the Γ-centered electron and H-centered hole octahedral Fermi surface segments, shown by the dashed arrow in Fig. 1(b) [22,23], stabilizes the IC SDW in bulk Cr [4–7]. Figure 1(c) shows a 3D band map of a thick chromium film in the Γ-H-P-N plane indicating the nesting that produces a Fermi surface incommensurability $\delta_{FS} = 0.05 \pm 0.005$, independent of d and T [21]. Hole doping in $Cr_{1-x}V_x$ alloys increases the size of the hole relative to the electron Fermi surface octahedron and thereby also increases δ_{FS} [5,24]. Figure 2(a) shows a 2D band map at $(x, d, T) = (0.00, 6\text{ nm}, 30\text{ K})$ along a line directly through the middle of the flat face of the electron octahedron indicated by the white line in Fig. 1(c). The intense band dispersing upward from the zone center ($k = 0$) would form the electron octahedron if it were not back-folded and split by the IC SDW [25–27]. Only the two lowest order IC folded bands exhibit measurable photoemission intensity [28,29]. This splitting, multiplied by a geometric factor, allows direct determination of the actual SDW commensurability δ_{SDW} [21]. In the limit probed in Fig. 2(a), $\delta_{SDW} = \delta_{FS}$. Upon increasing vanadium concentration, the measured incommensurability increases until $(x, \delta_{SDW}) \sim (0.035, 0.09)$ where the Néel transition to the paramagnetic phase is observed, as in Fig. 2(b). Our measured composition of the low temperature Néel transition agrees well with many measurements of bulk $Cr_{1-x}V_x$ alloys [5,30]. δ_{SDW} depends in a complicated way on x, d, and T and can depart significantly from δ_{FS}. Figure 2(c), for example, shows a band map for $(x, d, T) = (0.00, 3\text{ nm}, 30\text{ K})$, where only a single back-folded band is observed, corresponding to the C phase with $\delta_{SDW} = 0$ [21]. These data indicate that the IC phase is more stable in the thick-film limit, but a surface energetic interaction stabilizes the C phase in thinner films [21].

δ_{SDW} and the x-, d-, and T-induced transitions between the C, IC, and P phases can be visualized using images composed of the momentum distribution curves (MDC's). Each MDC is a constant-energy slice, averaging the back-folded region at a binding energy of 250 ± 100 meV. Figure 3(a) shows the smooth evolution of the splitting of the back-folded bands as a function of thickness for $x = 0.00$, $T = 30$ K. In thick films, the observed splitting corresponds to the bulk incommensurability, but it evolves smoothly to zero, corresponding to the C phase as the film thickness is reduced [21]. The MDC maps in Figs. 3(b) and 3(c) show the positions of back-folded bands as a function of vanadium concentration, for $T = 15$ K and $d = 2.5$ nm and 10 nm, respectively. The thin film [Fig. 3(b)] adopts the C phase for $x = 0$, transforms to the IC phase at x slightly above 0, and undergoes the Néel transition to the P phase at still higher x where the back-folded intensity disappears. The thicker film [Fig. 3(c)] starts IC at $x = 0$, becomes more incommensurate as x increases, and then undergoes the Néel transition. Assembling many MDC maps allows us to probe the C/IC/P-phase behavior in (x, d, T)-space, as shown by the dashed line in Fig. 4. The C-phase is favored at small d and higher T, the P phase dominates at above $x \sim 0.035$, and the IC phase is favored at low T and large d. These data demonstrate how the magnetic phase in

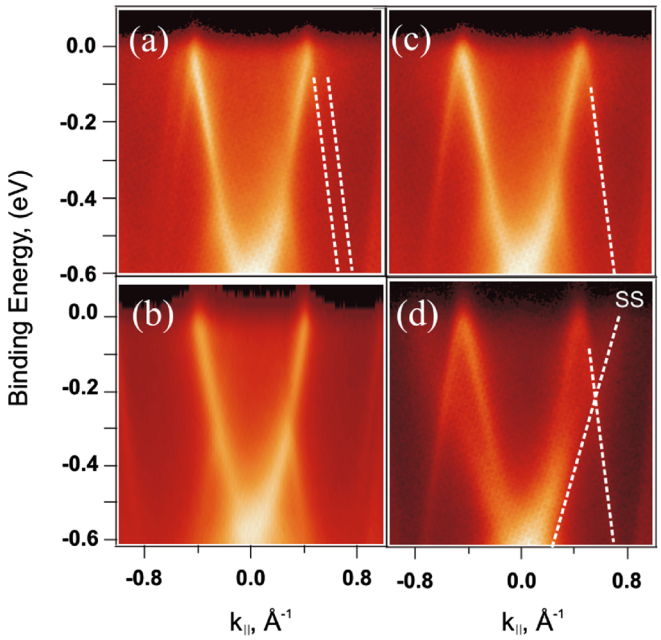

FIG. 2 (color online). 2D ARPES band maps showing energy band dispersion along a line directly through the face of the electron octahedron. (a) Pure Cr film of thickness $d = 6$ nm at $T = 30$ K showing two back-folded bands indicative of the IC phase. (b) Alloy film with $x = 0.06$ and $d = 6$ nm, $T = 30$ K, showing no back-folded band indicative of the P-phase. (c) Cr film of thickness $d = 3$ nm at $T = 30$ K showing one back-folded band indicative of the C phase. (d) Cr film of thickness $d = 6$ nm and $T = 30$ K with a monolayer of adsorbed hydrogen. The IC phase from panel (a) has transformed to the C phase, and a diffuse surface band has split from the bulk band as shown.

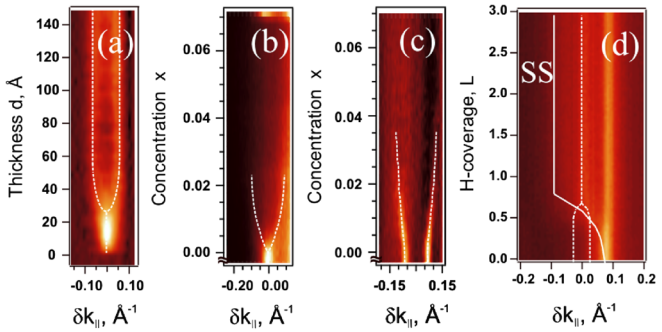

FIG. 3 (color online). MDC maps of the regions where the back-folded bands exist. (a) Cr at $T = 30$ K, as a function of film thickness d. The C phase at small d transforms to the IC phase at higher d. (b) and (c) Films at $T = 15$ K as a function of x, at $d = 2.5$ nm and $d = 10$ nm, respectively. The thin film (panel b) starts in the C phase and transforms quickly to the IC phase and then the P-phase as x increases, while the thick film starts IC and becomes more IC as the P phase is approached. Zero points on the thickness or concentration axes in Fig. 3 (a–c) correspond to beginning of wedges; below these points thickness/concentration is constant and equal to zero value. (d) Cr at $d = 6$ nm and $T = 30$ K as a function of hydrogen dose. The initially split back-folded band (IC) merges to form a single back-folded band (C), and over the same coverage regime a surface band splits from the intense bulk band edge and enters a projected band gap.

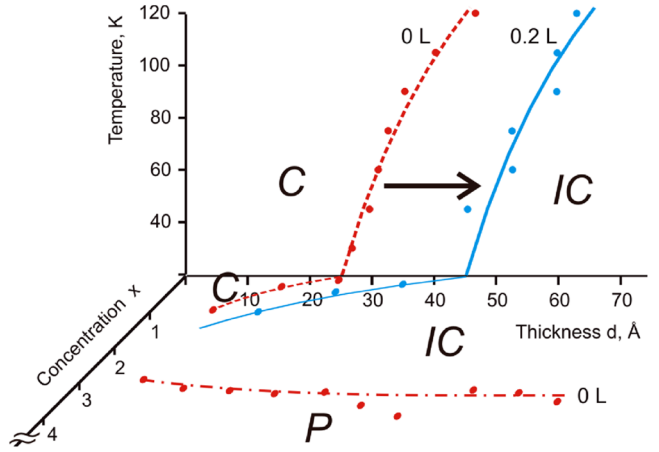

FIG. 4 (color online). Part of the low temperature 3D (x, d, T) magnetic phase diagram of clean (dashed line) and partially H-covered (solid line) $Cr_{1-x}V_x$ films as a function of x and d. Filled circles are measured transition points, and the various lines are guides to the eye. H-adsorption shifts the phase lines to higher thickness, indicating a surface-related preference for the C phase.

$Cr_{1-x}V_x$ thin films can be controlled with a static perturbation.

Figure 4 suggests that modification of the surface electronic structure might be used to control the SDW in thin films. An easy way to test this hypothesis is to study the impact of surface modification via dissociative hydrogen chemisorption. Figure 2(d) shows a band map at $(x, d, T) = (0.00, 6\text{ nm}, 30\text{ K})$ after saturating the outer Cr surface with a monolayer of hydrogen. Hydrogen adsorption removes several surface states and resonances (not seen in this figure), induces the emergence of a diffuse surface band from the bulk band edge of the electron octahedron, similar to previous results on W(110) and Mo(110) [31–33], and induces a transition from IC to C phase. The associated MDC map collected as a function of hydrogen coverage in Fig. 3(d) shows more clearly the evolution of the surface state and back-folded bulk bands. This phase change can be reversed by gently annealing to remove the adsorbed hydrogen. We also find that hydrogen adsorption on the outer surface extends the regime of C phase stability to thicker films, as shown by the solid line in Fig. 4. A small hydrogen coverage, estimated to be ~0.1 monolayer, produces an approximately rigid shift of the phase lines to larger d. The energetic interaction favoring C phase upon H-adsorption is very robust; we observe the C phase at a $x \sim 0.08$, about twice as high as where the bulk Néel transition occurs. The basis of this interaction is certainly surface-related and might be modification of the surface magnetic anisotropy [21] and/or a change in surface state nesting [24]. We note that the surface band moves into the band gap and thus becomes more surface-localized upon hydrogen adsorption, thereby presumably increasing the impact of the surface state. A recent paper suggests that electron-magnon coupling might be strong on this surface, though we are unable to reproduce those results in detail, and the observed coupling was to the bulk electron octahedron, not a surface state, in any case [34].

A concern is that we have used surface-sensitive photoemission experiments to draw conclusions about the magnetic phase of the entire film. Several observations justify our conclusions. First, the back-folded states are truly bulk states; the Fermi segments are those of the bulk Fermi surface [21,31–33,35]. Bulk and thin film states propagate to the surface, and it is common to make detailed conclusions about these states using photoemission. In the present case, δ_{SDW} converges on the known bulk incommensurability suggesting very strongly that we measure this parameter, not some surface-modified value. Moreover, the results presented here for $Cr_{1-x}V_x$ alloys determine a composition-dependence of the incommensurability in thick films that is similar to that in bulk alloys [5]. We do not see evidence for SDW-related gaps of the surface states, so there is no distinct surface magnetic periodicity. Finally, we have reproduced these results at many equivalent bulk Brillouin zones at photon energies from 21.2 through 500 eV and at various emission angles and a broad range of sampling depths. To interpret all of these results in terms of an exotic surface magnetic phase would be very difficult. This result is not surprising since any incommensurate ⟨100⟩-oriented SDW intersects a (110) interface with a spin structure that is itself incommensurate [17,21]. That will make the coupling between surface and bulk spin

structures very stiff since any change in spin structure near the surface will require many unfavorable local exchange interactions.

Therefore, our results prove that the electronic structure at the $Cr_{1-x}V_x$ surface can play a determining role in the thin film C-IC energetics. This may be viewed as a two step process: in the first step, magnetic structure of the surface layers is modified via controllable modification of the surface electronic structure, while in the second step, the magnetic exchange between the surface layers and bulk layers leads to modification of magnetic structure of the entire film. While hydrogen adsorption is not suitable for the dynamic control of the magnetic phase required for a real device, this system can be considered as a model demonstrating that control over the SDW is possible through the systematic modification of the surface electronic structure that might also be induced by application of an electric field in a field effect transistor (FET) geometry. Work function measurements suggest that each hydrogen atom induces a surface charge of order of 0.1 electron, which is not much higher than is achieved in a typical silicon FET.

An important technical advance in this work is the use of the composition wedges, which renders alloy composition a convenient nonthermal parameter that can be systematically varied in an experiment. Indeed, part of our motivation for pursuing the $Cr_{1-x}V_x$ alloy system was a recent discussion of non-Fermi-liquid (NFL) behavior near the quantum critical point that occurs when the Nèel temperature approaches 0 K [30,36–38]. Careful analysis of the electron distribution at the Fermi level reveals no evidence for the non-Fermi liquid behavior to an energy scale defined by instrumental resolution in the present experiment ($\Delta E \sim 30$ meV) at $T = 15$ K. Although our results do not support the assignment of non-Fermi liquid behavior, they should be considered primarily as setting an upper limit for the energy scale of interactions associated with the possible quantum critical behavior. We see many other fruitful applications for composition wedges in probing the properties of alloy thin films.

This work was supported by the US DOE under Grant No. DE-FG02-04ER46158. The ALS is operated under Contract No. DE-AC03-76SF00098 at Lawrence Berkeley National Laboratory.

[1] H. Ohno, D. Chiba, and F. Matsukura *et al.*, Nature (London) **408**, 944 (2000).
[2] D. Chiba, M. Yamanouchi, and F. Matsukura, *et al.*, Science **301**, 943 (2003).
[3] S. T. B. Goennenwein, T. A. Wassner, and H. Huebl *et al.*, Phys. Rev. Lett. **92**, 227202 (2004).
[4] E. Fawcett, Rev. Mod. Phys. **60**, 209 (1988).
[5] E. Fawcett, H. L. Alberts, and V. Y. Galkin *et al.*, Rev. Mod. Phys. **66**, 25 (1994).
[6] A. W. Overhauser, Phys. Rev. Lett. **4**, 462 (1960).
[7] A. W. Overhauser, Phys. Rev. **128**, 1437 (1962).
[8] P. Bödeker, P. Sonntag, and A. Schreyer, *et al.*, J. Appl. Phys. **81**, 5247 (1997).
[9] R. S. Fishman and Z.-P. Shi, Phys. Rev. B **59**, 13849 (1999).
[10] E. E. Fullerton, S. Adenwalla, and G. P. Felcher *et al.*, Physica B (Amsterdam) **221**, 370 (1996).
[11] J. Meersschaut, J. Dekoster, and R. Schad *et al.*, Phys. Rev. Lett. **75**, 1638 (1995).
[12] A. M. N. Niklasson, B. Johansson, and L. Nordström, Phys. Rev. Lett. **82**, 4544 (1999).
[13] A. Schreyer, C. F. Majkrzak, and T. Zeidler *et al.*, Phys. Rev. Lett. **79**, 4914 (1997).
[14] P. Sonntag, P. Bödeker, and T. Thurston *et al.*, Phys. Rev. B **52**, 7363 (1995).
[15] F. Y. Yang and C. L. Chien, Phys. Rev. Lett. **90**, 147201 (2003).
[16] H. Zabel, J. Phys. Condens. Matter **11**, 9303 (1999).
[17] K.-F. Braun, S. Fölsch, and G. Meyer *et al.*, Phys. Rev. Lett. **85**, 3500 (2000).
[18] H. Fritzsche, S. Bonn, and J. Hauschild *et al.*, Phys. Rev. B **65**, 144408 (2002).
[19] H. Fritzsche, S. Bonn, and J. Hauschild *et al.*, Eur. Phys. J. B **36**, 175 (2003).
[20] J. Meersschaut, J. Dekoster, and S. Demuynck *et al.*, Phys. Rev. B **57**, R5575 (1998).
[21] E. Rotenberg, B. K. Freelon, and H. Koh *et al.*, New J. Phys. **7**, 114 (2005).
[22] T.-S. Choy, J. Naset, and J. Chen *et al.*, Bull. Am. Phys. Soc. **45(1):L36**, 42 (2000).
[23] T. S. Choy, http://www.phys.ufl.edu/fermisurface/.
[24] O. Krupin, E. Rotenberg, and S. D. Kevan (to be published).
[25] R. S. Fishman and S. H. Liu, Phys. Rev. B **50**, 4240 (1994).
[26] R. S. Fishman and S. H. Liu, Phys. Rev. B **54**, 7252 (1996).
[27] R. S. Fishman and S. H. Liu, Phys. Rev. Lett. **76**, 2398 (1996).
[28] E. Rotenberg, W. Theis, and K. Horn *et al.*, Nature (London) **406**, 602 (2000).
[29] J. Voit, L. Perfetti, and F. Zwick *et al.*, Science **290**, 501 (2000).
[30] A. Yeh, Y.-A. Soh, and J. Brooke *et al.*, Nature (London) **419**, 459 (2002).
[31] E. Rotenberg, J. W. Chung, and S. D. Kevan, Phys. Rev. Lett. **82**, 4066 (1999).
[32] E. Rotenberg and S. D. Kevan, Phys. Rev. Lett. **80**, 2905 (1998).
[33] E. Rotenberg, J. Schaefer, and S. D. Kevan, Phys. Rev. Lett. **84**, 2925 (2000).
[34] F. Schiller, D. V. Vyalikh, and V. D. P. Servedio *et al.*, Phys. Rev. B **70**, 174444 (2004).
[35] J. Schäfer, E. Rotenberg, and S. D. Kevan *et al.*, Phys. Rev. Lett. **83**, 2069 (1999).
[36] M. Lee, A. Husmann, and T. F. Rosenbaum *et al.*, Phys. Rev. Lett. **92**, 187201 (2004).
[37] M. R. Norman, Q. Si, and Y. B. Bazaliy *et al.*, Phys. Rev. Lett. **90**, 116601 (2003).
[38] C. Pépin and M. R. Norman, Phys. Rev. B **69**, 060402 (2004).